Wind in Weak Grids: 4 Hz or 30 Hz Oscillations?

Lingling Fan, *Senior Member, IEEE*, and Zhixin Miao, *Senior Member, IEEE*

***Abstract*—With wind being integrated into weak grids, Texas sees 4 Hz oscillations while China's west region sees 30 Hz oscillations. While both phenomena have been studied and are claimed to be due to weak grid wind integration, it is valid to ask this question: What causes the significant difference in oscillation frequencies? In this letter, we offer an explanation and provide evidences through dynamic modeling and eigenvalue analysis. One of the possible reasons is identified as phase-locked-loop parameters. Furthermore, both the low-frequency and subsynchronous-frequency modes exist at the same time for Type-4 wind with dc-link voltage control.**

***Index Terms*—Wind, PLL, oscillations.**

I. Introduction

With wind being integrated into weak grids, Texas sees 4 Hz oscillations [1]. Low-frequency oscillations have also been observed in high voltage direct current (HVDC) systems where voltage source converters are connected to a weak ac grid [2], [3]. In [2], oscillations with frequencies less than 4 Hz are observed when short circuit ratio (SCR) reaches 1.6. In [3], less than 4 Hz oscillations are identified due to low SCR. Since 2014, China's Xinjiang region sees 30 Hz oscillations [4] due to Type-4 wind integration. The oscillation frequency can vary from 20 Hz to 40 Hz depending on the operation condition [4]. This type of oscillation is termed as subsynchronous frequency oscillation.

While both phenomena have been studied and are claimed to be due to weak grid wind integration, it is valid to ask this question: What causes the significant difference in oscillation frequency?

In this letter, we examined different converter control assumptions and parameter selections in the literature. We built analytical models for Type-4 wind with weak grid interconnection and carried out eigenvalue analysis as well as dynamic simulation to show the difference in converter control, particularly PLL parameters, causes the significant difference in oscillation frequencies.

We found that the low-frequency mode and the subsynchronous-frequency mode are two different modes existing at the same time. PLL parameters play a big role in determining which mode is dominant. Further, the co-existence of the two modes will not appear should dc-link dynamics and dc-link voltage control are not modeled.

II. Dynamic Models

The study system is shown in Fig. 1. Output power is assumed at the nominal level or 1 pu and the PCC voltage at steady-state is 1 pu. Shunt compensation is included to provide 25% nominal level reactive power.

Two types of converter controls will be examined. The difference lies in whether active power control or dc-link voltage control is assumed.

Manuscript received April 9, 2018; revised June 2, 2018; accepted June 26, 2018. Date of publication July 4, 2018; date of current version August 22, 2018. Paper no. PESL-00073-2018. *(Corresponding author: Lingling Fan.)*

The authors are with the Department of Electrical Engineering, University of South Florida, Tampa, FL 33620 USA (e-mail: linglingfan@usf.edu; zhixin.miao@ieee.org).

Color versions of one or more of the figures in this paper are available online at http://ieeexplore.ieee.org.

Digital Object Identifier 10.1109/TPWRS.2018.2852947

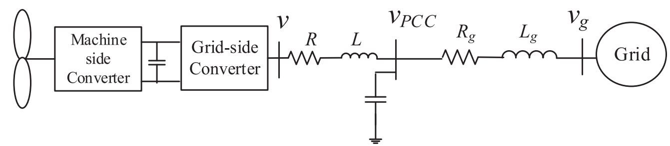

Fig. 1. Circuit diagram of the system.

Investigation on HVDC with weak grid connection [2], [3] assumes active power control. While investigation on Type-4 wind weak grid interconnection [4], [5] assumes dc-link voltage control. [4] indicates that the dc-link capacitor dynamics is related to the subsynchronous-frequency mode through participation factor analysis.

Therefore, two dynamic models have been examined: active power control (Model 1) versus dc-link voltage control (Model 2). For Model 1, dc-link dynamics are ignored. In Model 2, dc-link dynamics are included. Details regarding Model 1 can be found in the authors' prior work [6]. Parameters in [6] are adopted for this project.

Model 2 includes dc-link dynamics, converter vector control, PLL and grid dynamics (shunt capacitor, transmission line inductor). All dynamics are modeled based on dq-reference frames so that small-signal analysis is possible. The modeling block diagram of the system is shown in Fig. 2a.

The dc-link dynamics is described as follows.

$$\frac{CV^2_{\mathrm{base,dc}}}{2P_{\mathrm{base}}}\frac{dV^{2\mathrm{pu}}_{\mathrm{dc}}}{dt} = P^{\mathrm{pu}}_{\mathrm{wind}} - P^{\mathrm{pu}} \tag{1}$$

where P is the active power leaving the converter to the grid, P_{wind} is the wind power and treated as a known parameter in the dynamic model. V_{dc} is the dc-link voltage. Superscript "pu" notates per unit variables. The parameter $\tau = \frac{CV^2_{\mathrm{base,dc}}}{2P_{\mathrm{base}}}$ (0.0272) is computed based on the parameters of a 2 MW Type-4 wind from MATLAB Simscape: nominal dc link voltage 1100 V, capacitor size 0.09 F. Vector control is adopted with V^2_{dc} control for the d-axis control and the PCC voltage control for the q-axis control.

III. Eigenvalue Analysis and Simulation Results

Based on the two dynamic models, four sets of PLL parameters are examined. The grid reactance X_g varies from 0.25 pu to 0.59 pu with a step size 0.02 pu. Bode plots of the closed-loop transfer functions of the PLLs, bandwidths, parameters are presented in Fig. 2b.

Eigenvalue loci of Model 1 are shown in Fig. 3 while eigenvalue loci of Model 2 are shown in Fig. 4. Model 1 has only one mode moving to the right half plane (RHP) when the grid strength reduces while Model 2 shows two modes moving to the RHP. Model 1 appears to have more stability margin compared to Model 1.

Time-domain simulation results of Model 2 are presented in Fig. 5. A same operating condition is used: $X_g = 0.55$ pu. Four PLLs are examined. for At $t = 1$ s, the dc-link voltage squared reference has a 0.01 pu step change. At 2.5 second, the wind power is ramped down to

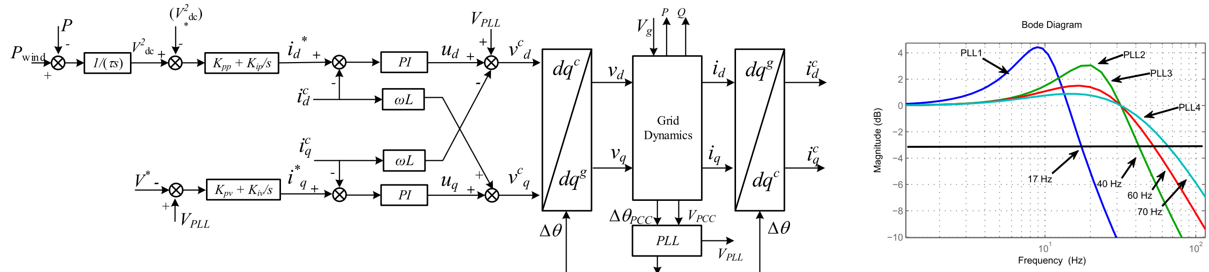

Fig. 2. (a) Block diagram of the system model. (b) Bode plots for four PLLs used in the R1 version. $K_{p,\mathrm{PLL}}$ and $K_{i,\mathrm{PLL}}$ for the four PLLs are: PLL1 (50, 4000); PLL2 (150, 20000); PLL3 (250, 20000), PLL4 (350, 20000). Their respective bandwidths are 17 Hz, 40 Hz, 60 Hz, and 70 Hz.

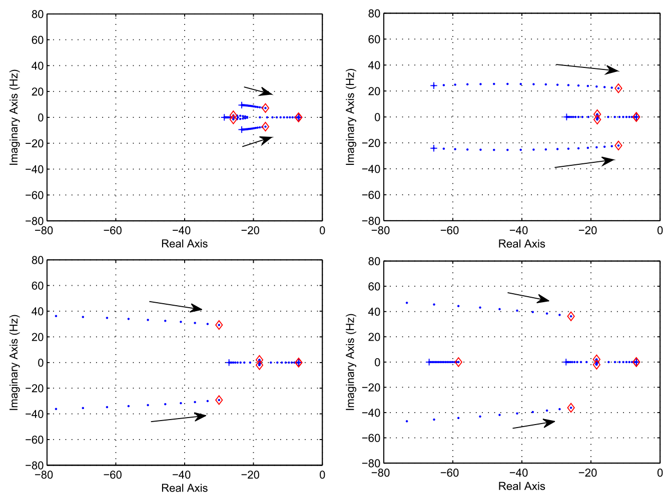

Fig. 3. Model 1 eigenvalue loci.

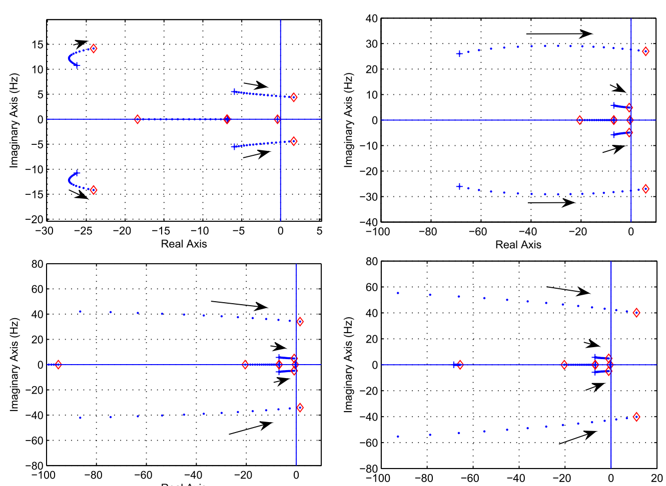

Fig. 4. Model 2 eigenvalue loci.

have a 50% reduction. This ramp down is simulated by passing a step response through a first-order unit $\frac{1}{2.5s+1}$.

It can be seen that for PLL1, when there is a change in dc-link voltage squared reference, 4.5 Hz undamped oscillations appear. For PLL2, 30 Hz oscillations are dominant. The low-frequency mode can also be seen in the initial few cycles. Reducing the wind power suppresses the 30 Hz oscillations damped. For the PLL3 case, both modes have

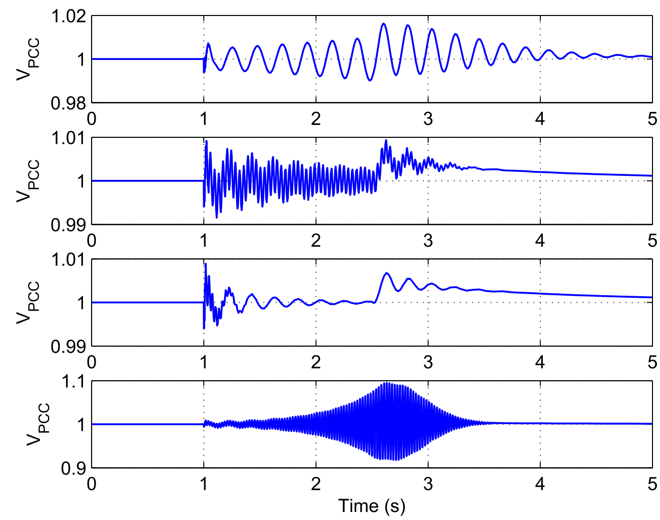

Fig. 5. Simulation results. From upper to bottom: PLL1, PLL2, PLL3, and PLL4.

adequate damping. For the PLL4 case, the 40 Hz oscillation mode is dominant and makes the system is unstable. Ramping down wind power suppresses the oscillations. The simulation results corroborate with the eigenvalue analysis.

In summary, we successfully demonstrate the co-existence of low-frequency and subsynchronous-frequency oscillation modes. Further, PLL parameters play a big role in determining which mode is dominant.

References

[1] S.-H. Huang, J. Schmall, J. Conto, J. Adams, Y. Zhang, and C. Carter, "Voltage control challenges on weak grids with high penetration of wind generation: Ercot experience," in *Proc. IEEE Power Energy Soc. General Meeting*, 2012, pp. 1–7.

[2] J. Z. Zhou, H. Ding, S. Fan, Y. Zhang, and A. M. Gole, "Impact of short-circuit ratio and phase-locked-loop parameters on the small-signal behavior of a VSC-HVDC converter," *IEEE Trans. Power Del.*, vol. 29, no. 5, pp. 2287–2296, Oct. 2014.

[3] L. Papangelis, M.-S. Debry, T. Prevost, P. Panciatici, and T. Van Cutsem, "Stability of a voltage source converter subject to decrease of short-circuit capacity: A case study," in *Proc. 20th Power Syst. Comput. Conf.*, 2017, pp. 1–7.

[4] H. Liu *et al.*, "Subsynchronous interaction between direct-drive PMSG based wind farms and weak ac networks," *IEEE Trans. Power Syst.*, vol. 32, no. 6, pp. 4708–4720, Nov. 2017.

[5] K. M. Alawasa, Y. A.-R. I. Mohamed, and W. Xu, "Modeling, analysis, and suppression of the impact of full-scale wind-power converters on subsynchronous damping," *IEEE Syst. J.*, vol. 7, no. 4, pp. 700–712, Dec. 2013.

[6] L. Fan, "Modeling type-4 wind in weak grids," *IEEE Trans. Sustain. Energy*, to be published, doi: 10.1109/TSTE.2018.2849849.